Environmental Pollution 261 (2020) 114157

Contents lists available at ScienceDirect

Environmental Pollution

journal homepage: www.elsevier.com/locate/envpol

Simultaneous removal of arsenic, cadmium, and lead from soil by iron-modified magnetic biochar☆

Xiaoming Wan [a, b, *], Chongyang Li [b], Sanjai J. Parikh [b]

[a] Institute of Geographic Sciences and Natural Resources Research, Chinese Academy of Sciences, Beijing, 100101, China
[b] Department of Land, Air and Water Resources, University of California, Davis, CA, 95616, USA

ARTICLE INFO

Article history:
Received 16 December 2019
Received in revised form
30 January 2020
Accepted 8 February 2020
Available online 11 February 2020

Keywords:
Arsenic
Biochar
Cadmium
Lead
Magnetite
Sawdust

ABSTRACT

Effective and economically viable method to remove elevated metal(loid)s from farm and industrial lands remains a major challenge. In this study, magnetic biochar-based adsorbents with Fe_3O_4 particles embedded in a porous biochar matrix was synthesized via iron (Fe) treated biochar or thermal pyrolysis of Fe treated cedar sawdust. Application and separation of the adsorbent to a multi-contaminated soil slurry simultaneously removed 20–30% of arsenic, cadmium and lead within 24 h. Fast removal of multi-metal(loid)s result from the decrease in all operationally defined fractions of metal(loid)s, not limited to the exchangeable fraction. The direct removal of arsenic-enriched soil particles was observed via micro X-ray fluorescence maps. Furthermore, through comparison of biochars with different production methods, it has been found that magnetization after pyrolysis treatment leads to stronger metals/metalloids adsorption with a higher q_e (bound sorbate) than other treatments but pyrolysis after magnetization stabilized Fe oxides on the biochar surface, indicating a higher biochar recovery rate (~65%), and thus a higher metal(loid)s removal efficiency. The stability of Fe oxides on the surface of biochar is the determining factor for the removal efficiency of metal(loid)s from soil.

1. Introduction

Metal(loid)s contamination in soil is a global problem (Komarek et al., 2013; Toth et al., 2016). Due to mining activities, the application of metal(loid)s-enriched products to soil, and atmospheric deposition, toxic metal(loid)s have been released into the environment (Chen et al., 2018a). Soil is an important sink of metal(loid)s and one of the principal sources for their uptake in crops (Gil et al., 2018). In addition, metal(loid)s in soil can be a source of water or air pollution due to runoff and airborne dust, respectively (Rai et al., 2019; Shajib et al., 2019; Tian et al., 2019). Arsenic (As), cadmium (Cd) and lead (Pb) are three of the most concerning contaminants due to their wide distribution and high toxicity (Kim et al., 2009; Li et al., 2016; Norton et al., 2014).

A range of soil remediation technologies have been applied with varying levels of success; either to remove metal(loid)s from the contaminated medium or to reduce their bio-toxicity (Khalid et al., 2017). Among these technologies, phytoextraction and immobilization are currently the most common, but also have substantial drawbacks. Phytoextraction requires a long time (de Abreu et al., 2012), and usually only removes one single element at one time due to the specificity of hyperaccumulators to a certain element (Kumar et al., 1995), although there are also exceptions which used high-biomass plants to deal with multi-contaminated soil (de Abreu et al., 2012). Immobilization is an economical and easy way to decrease the bioavailability of metal(loid)s in soil; however, the long-term effect of immobilizers application to soil and the potential of contaminants release back to soil or water has not be fully explored (Vitkova et al., 2017). New methods for the efficient extraction of multiple inorganic contaminants simultaneously from soil are required.

Despite potential drawbacks to biochar, if not used prudently (Gelardi et al., 2019; Li et al., 2018), biochar still holds great potential due to its potential of waste recycling, ease of production, economic efficiency, and benefits for agronomic and environmental applications (Gonçalves et al., 2018; Igalavithana et al., 2019). One of the potential environmental functions is to decrease the mobility or bio-availability of heavy metals in soil or water systems, such as Cd and Pb, depending on its high surface area, the cation exchange

☆ This paper has been recommended for acceptance by Philip Smith.

* Corresponding author. Institute of Geographic Sciences and Natural Resources Research, Chinese Academy of Sciences, Beijing 100101, China.
E-mail address: wanxm.06s@igsnrr.ac.cn (X. Wan).

https://doi.org/10.1016/j.envpol.2020.114157
0269-7491/

capacities (O'Connor et al., 2018; Palansooriya et al., 2020), and the enrichment of some special metals stabilizing element such as phosphorus (Netherway et al., 2019). However, the liming effect of biochar usually increases the mobility of metalloids (Beesley and Marmiroli, 2011; Beesley et al., 2011). The combination of biochar with other soil amendments, or the modification of biochar with novel structures and surface properties are strategies suggested to improve the multi-metal(loid)s remediation efficacy (Beesley and Marmiroli, 2011; Zhang et al., 2013). Among these combinations, biochar/metal composite showed strong potential (Zhang et al., 2020). An Fe and calcium modified magnetic biochar can remove 98% of Cd(II) and 85% of As(III) from an aqueous system (Wu et al., 2018). The application of zero-valent iron and biochar effectively immobilized metal(loid)s in paddy soil, decreasing the As concentration in the rice grain by 61% (Qiao et al., 2018). Use of a magnetic biochar reduced the acid-soluble concentrations of Cd, Zn and Cu by 8–10%, 27–29%, and 59–63%, respectively (Lu et al., 2018). Such mitigation of toxic elements accumulation in crops using biochar has been further confirmed in field experiments (Xing et al., 2019).

In the current study, Fe oxide modified biochar was used to remove multi-metal(loid)s from a soil slurry system. It is hypothesized that magnetic biochar produced by Fe modification, which takes merits of the unique properties of both biochar (high sorption capacity for cations, e.g., Cd) and iron oxide (high sorption capacity for As), can increase its sorption capacity of multi-metal(loid)s from soils, given its success in aqueous experiments (Wu et al., 2018). In addition, the magnetic property of Fe modified biochar may permit the separation of biochar from soil, thus efficiently remove multi-metal(loid)s.

Several biochars were produced through different procedures and utilized as adsorbents in soil metal(loid)s removal experiment and aqueous adsorption experiment. The relationship was to be disclosed between the two involved processes (adsorption of multi-metal(loid)s to biochar, and the separation of contaminants-enriched biochar from soil) and the morphological and physio-chemical properties of biochar, aiming to find the determining factors for the metal(loid)s removal efficiency using magnetic biochar, which can provide further guidance on the optimization of magnetic biochar production procedure.

2. Experimental section

2.1. Soil and biochar

Soil samples were collected from the Providence Quartz Mill Site in Nevada City, California, (USA), with the center located at latitude 39.259°, and longitude −121.038°. Providence Mine operated between the 1860s and 1920. A total of over $20 million in gold was produced by the mine in that period. With funding from Sierra Nevada Conservancy Assessment Grant and a US EPA Brownfields cleanup grant, this site was under a procedure to characterize and mitigate recognized environmental conditions. This area has a Mediterranean climate, with hot and dry summers, and is vegetated with fir, oak, cedar and pine trees and various underbrush including honeysuckle, Himalayan blackberry and poison oak. The geology is mainly quartz diorite and granodiorite. The soil at this site is primarily (85%) mapped as the Musick Series (United States Department of Agriculture [USDA] classification: fine-loamy, mixed, semi active, mesic ultic haploxeralf). About 5 kg soil (sandy loam to sandy clay loam) was taken from the upper layer (0–30 cm) after removal of vegetation. Plant material was removed, and the remaining soil was homogenized on site and in the laboratory. The soil was air-dried and sieved to 2 mm before further experiment. Soil properties are provided in Table 1. To simulate paddy soil, soil slurry was made by mixing soil with 18.2 MΩ-cm water (Barnstead Nano pure; BNP) at a ratio of 3:2 (v/v) for one month, and then freeze-dried for later incubation experiment and chemical analysis. The total concentrations of As, Cd and Pb of the soil were 47.3 ± 6.7 mg kg^{-1}, 12.1 ± 4.4 mg kg^{-1}, and 729 ± 92 mg kg^{-1}, respectively, exceeding the DTSC-recommended screening levels for residential soil (0.11 mg As kg^{-1}, 5.2 mg Cd kg^{-1}, and 80 mg Pb kg^{-1}) established by the Department of Toxic Substances Control, California Environmental Protection Agency (HERO, 2016).

Three production procedures were used to produce different magnetized biochars: (1) pyrolysis before magnetizing the biochar (indicated as PM treatment); (2) pyrolysis after magnetizing the biomass (indicated as MP treatment); and (3) pyrolysis conducted twice, once before magnetizing and again after magnetizing (indicated as PMP treatment). The raw biochar without any magnetizing process was indicated as P treatment. Biomass used in the current study was red cedar (*Thuja plicata*) sawdust.

During the entire pyrolysis and cooling process, the furnace was under N_2 atmosphere. Furnace temperature was increased from room temperature (24 ± 1 °C) to 300 °C at the rate of ~3 °C per min, and then held at 300 °C for 2 h. The pyrolysis temperature was set at 300 °C for two reasons: (1) the Curie temperature of Fe_3O_4 is 500–566 °C (Kolhatkar et al., 2017); (2) within the commonly used pyrolysis temperatures lower than the Curie point of Fe_3O_4 (Li et al., 2020), 300 °C showed a higher comprehensive removal rate of all the three metal(loid)s in our preliminary experiments (Fig. S1).

During magnetization, 20 g biochar or biomass was suspended in 200 mL BNP water, and then mixed with magnetizing solution made by adding $FeCl_3 \cdot 6H_2O$ (20 g) and $FeSO_4 \cdot 7H_2O$ (11.1 g) with 600 mL BNP water. NaOH (10 M) was added dropwise into the mixed suspension to adjust the pH to ~10. The mixed suspension was boiled at 80 °C for 1 h, and then a magnet was used to separate biochar or biomass from the suspension. The biochar or biomass was rinsed with BNP water and ethanol three times and dried at 70 °C for 12 h. Properties of biochar are provided in Table 2. The detailed analytical methods of biochar characteristics have been presented elsewhere (Mukome et al., 2013).

2.2. Metal(loid)s removal from soil and aqueous systems

In the soil experiment, magnetic biochar was mixed with the soil slurry, with a water to solid ratio of 3:1 (w:w). In the solid, the ratio of biochar to soil is 1:10 (w:w). After ~24 h, the biochar was separated from soil suspension and rinsed three times with BNP water and methanol. During the separation, a Grade N52 Neodymium magnet (UNSPSC Code 24,100000) was applied to the outside of the slurry container for 10 s. And then the magnet was slowly lifted upwards, with the biochar particles within the container moving upwards with the force from the outside magnet. A plastic spoon was used to remove the biochar particles at the top edge of the container. For each sample, this process was repeated for three times. The separated biochar (recovery rate ranging from 45% to 65%) and the remaining soil fractions were freeze-dried for the sequential extraction and total concentration analysis of As, Cd, and Pb. There are three replicates for each treatment.

In the aqueous experiment, 0.01 g biochar (raw or magnetic) was added to 20 mL solution containing single metal(loid) or combination of metal and metalloid. Arsenic was added in form $NaAsO_2$ $5H_2O$, Cd in form of $CdCl_2$ $2.5H_2O$, and Pb in form of $Pb(NO_3)_2$ at the concentration of 8 mg L^{-1} individually for each metal(loid). pH was adjusted to 6.0. The 50-mL centrifuge tubes were placed on a rotating shaker and oscillated at 250 rpm for different durations. After ~24 h, the biochar was separated from solution using 0.45 μm filter. The filtrate was analyzed for the total concentrations of metal(loid)s. There are three replicates for each

Table 1
Properties of soils used in the experiment.

Soil	pH	Sand (%)	Silt (%)	Clay (%)	TOC (%)	P (total, %)	K (total,%)	NH_4–N (mg/kg)	NO_3–N (mg/kg)	Bray-P (mg/kg)	Olsen-P (mg/kg)	SO_4–S (mg/kg)
Before	5.4	54	26	20	2.8	0.12	0.16	2.2	1.8	3.9	3.9	143
After PM	5.8	55	27	18	3.3	0.12	0.14	3.5	0.8	3.2	4.5	121
After PMP	5.8	56	26	18	3.2	0.12	0.15	4.3	0.6	2.8	5.4	110
After MP	5.6	56	26	18	3.0	0.12	0.16	3.2	0.6	3.8	4.2	133

Before indicates the soil before the application of biochar; After PM, After PMP, and After MP indicate the soil after PM, PMP, and MP biochar adsorption and separation, respectively. PM indicates the biochar produced by magnetization after pyrolysis; PMP indicates the biochar produced by pyrolysis twice, once before magnetizing and again after magnetizing; MP indicates the biochar produced by pyrolysis the magnetized biomass. pH: reactivity in KCl; TOC: the organic carbon content [%].

Table 2
Properties of biochars produced in the experiment.

	pH	C(%)	N(%)	Ash(%)	Fe(%)	$S_{BET}(m^2/g)$	$S_{mic}(m^2/g)$	$V_p(cm^3/g)$	$V_{mic}(cm^2/g)$
P	6.3	81.3	0.13	22.5	0.08	533	418	0.095	0.093
PM	9.7	62.1	0.16	26.9	27.9	370	288	0.077	0.070
PMP	10.3	53.9	0.30	36.8	37.5	343	266	0.062	0.059
MP	10.0	44.5	0.08	44.5	48.7	257	191	0.040	0.038

pH: reactivity in 0.1 M KCl; C, N: elemental composition [%]; Ash: ash content [%]; S_{BET}: surface area; S_{mic}: micropore area; V_p: total pore volume; V_{mic}: micropore volume. P indicates the raw biochar without magnetization; PM indicates the biochar produced by magnetization after pyrolysis; PMP indicates the biochar produced by pyrolysis twice, once before magnetizing and again after magnetizing; MP indicates the biochar produced by pyrolysis the magnetized biomass.

treatment. A separate batch adsorption kinetics experiment was conducted on the PM and PMP biochar, details of which are described in the supplementary material.

2.3. Recovery of magnetic biochar from soil

The recovery rate of biochar was calculated by quantifying the biochar content in the soil before and after its separation from soil via a magnet. Specific markers for biochar, benzene polycarboxylic acids (BPCAs), were used to estimate the biochar content within soil (Li et al., 2018; Wiedemeier et al., 2013). In brief, soil with a known total organic carbon content (TOC) was digested with nitric acid (68–70%, 8 h at 170 °C). The resulting BPCA solution was filtered, purified, and analyzed using HPLC. Biochar specific conversion factor, the reciprocal of the ratio of BPCA carbon to TOC, was adopted from an earlier study to calculate the content of biochar in the soil (Li et al., 2018).

2.4. Characteristics analysis of biochar

Biochar samples before the experiment and separated from the soil and aqueous experiments were characterized for the morphology, porosity, and magnetic property. Physical analysis of the biochar was conducted by Micromeritics' Particle Testing Authority by performing CO_2 adsorption– desorption isotherms at 273.15 K using a TriStar II Plus 3.00 according to ISO9277. The specific surface area (S_{BET}) of the biochar was determined according to the Brunauer – Emmett – Teller isotherm. The microscopic features of the biochar were characterized by a scanning electron micro-scope (FEI Scios DualBeam FIB/SEM, USA) equipped with an Oxford X-Max Energy Dispersive X-ray Spectroscopy (EDS) Detector. The X-ray diffraction (XRD) analysis was conducted to identify crystallographic structures of the samples using an X-ray diffractometer (UltimaIV, Japan) using a Cu X-ray source at 40 kV and 40 mA. Biochar samples were ground to the size of <40 μm before analysis. The samples were scanned from 3 to 65° with the scan speed of 2° min^{-1}. MDI Jade 6.5 software with PDF 2 database was used to analyze the XRD data. Attenuated total reflectance (ATR) Fourier transform infrared (FTIR) spectroscopy was used to evaluate the chemical properties of the raw and magnetized biochar on a Thermo Nicolet 6700 spectrophotometer with a single bounce diamond ATR accessory (GladiATR, PIKE Technologies, Madison, WI) and DTGS detector at ambient temperature (23 ± 1 °C). The magnetic moment versus magnetic field hysteresis loops of different biochars were measured with a Magnetic measuring system (MPMS-3, Quantum Design Company, America) at ambient temperature (23 ± 1 °C).

2.5. Chemical analysis methods

The aqua regia method was used to digest soil samples, for the measurement of the total As, Cd, and Pb concentrations before and after the application of biochar. Digestion blanks and a loam soil reference material (ERM CC141) were carried through the digestion process for quality control and recovery assurance. The concentrations of total As, Cd, and Pb were determined by ICP-MS (PerkinElmer 600X, USA). Calibration curve accuracy was confirmed by certified reference material (1640a). Sequential extraction of As from soil samples before and after the experiment was conducted using five-step sequential extraction method according to Wenzel et al. (2001); sequential extraction of Cd and Pb was conducted according to Tessier et al. (1979).

Synchrotron radiation (SR) based micro X-ray fluorescence (XRF) mapping was used to obtain the micro-distribution of As on biochar, compared with the distribution of Fe. Based on the results of micro-XRF, As K-edges X-ray absorption near edge structure (XANES) was conducted on regions of elevated As, to obtain As speciation. Experiments were conducted on beamline 10.3.2, Advanced Light Source, Lawrence Berkeley National Laboratory, US.

2.6. Statistics

PASW® Statistics 18.0 was used to statistically analyze data. Significance level was set at an error probability of 0.05. Origin 9.0 was used to make the graphics. Differences in metal(loid)s removal rate among treatments were tested using ANOVAs (Tukey). Values represent mean ± standard deviation (n = 3).

3. Results

3.1. Removal of metal(loid)s by magnetized biochar from soil and aqueous system

After incubation with the magnetized biochars for 24 h,

followed by the separation of biochar from soil using a magnet, the total concentrations of As, Cd and Pb significantly decreased (Fig. 1a). PMP treatment showed the highest removal rate of 28%, 25% and 32% for As, Cd and Pb, respectively. PM treatment also indicated high removal rate for As and Pb, being 23% and 24%, respectively, but removed less Cd (16.9%). MP treatment decreased the Cd concentration by ~23% but removed less As (4.7%) and Pb (15.1%).

In comparison with the soil experiments, aqueous experiments revealed that MP had the highest As removal among the three magnetic biochar treatments (Fig. 1b), in accordance with the highest Fe content of MP treatment (Table 2). PM treatment showed the highest Cd and Pb removal (Fig. 1b), in accordance with its highest carbon content (C%) and highest BET surface area (Table 2). All the three magnetic biochar showed higher metal(loid)s removal than the raw biochar (P treatment) with much lower pH value. Batch adsorption kinetics experiment found that the magnetized biochar showed a faster and stronger adsorption of Cd and Pb than As, indicated by higher adsorption capacity and shorter equilibrium times (Figs. S2–S4, Table S1). Compared to the respective PMP treatment, PM treatment showed a ~65% higher adsorption capacity of As (Table S1). The co-existence of As in the dual-adsorbate system decreased the adsorption of Cd to magnetic biochars, compared to the single-adsorbate system of Cd (Fig. S2). However, such negative effect of As on the adsorption of Pb, or the negative effect of Cd or Pb on the adsorption of As was not observed.

Sequential extraction results indicated that all the five fractions of Cd and Pb in the experimental soil decreased to a certain extent, with extractable fraction (F1) being the main removed fractions (Fig. 2). The F1 fractions of Cd decreased by 29.3% and 41.0% by PM and PMP treatment after the removal experiment. The F1 fractions of Pb decreased by 61.7% and 63.9% by PM and PMP treatment after the removal experiment. The fractions of Cd and Pb bound to carbonates (F2) also showed apparent decrease. Arsenic showed different extents of decrease in all five fractions. PM treatment showed the biggest reduction in the non-specifically sorbed fraction (F1), while PMP treatment showed no significant difference among different fractions.

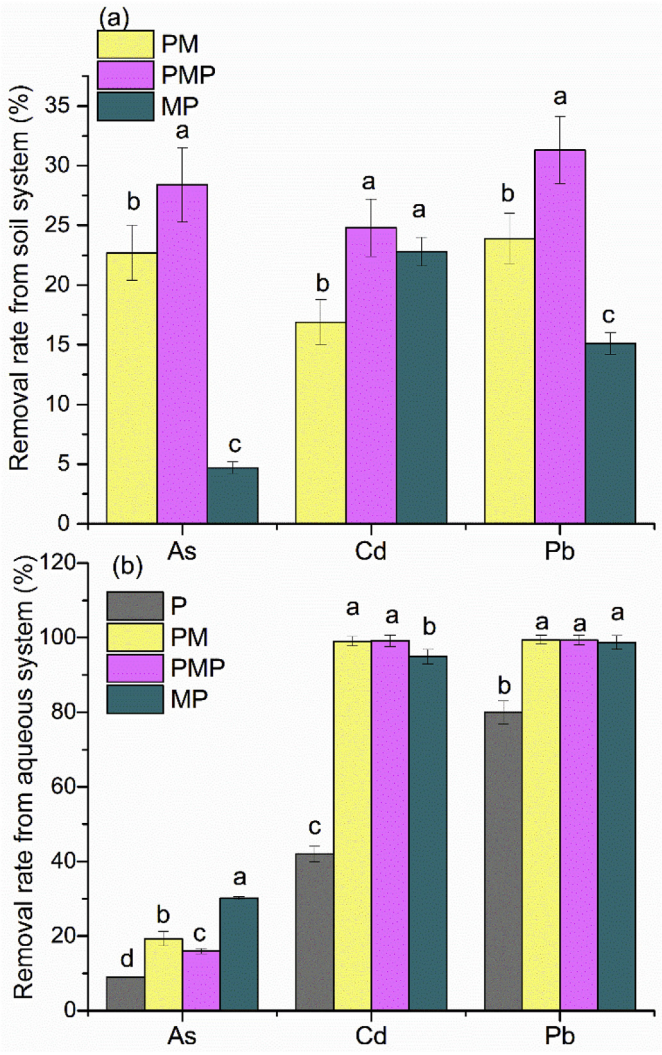

Fig. 1. Removal rates of As, Cd and Pb by biochars from soil (a) and aqueous (b) system. P indicates the raw biochar without magnetization; PM indicates the biochar produced by magnetization after pyrolysis; PMP indicates the biochar produced by pyrolysis twice, once before magnetizing and again after magnetizing; MP indicates the biochar produced by pyrolysis the magnetized biomass. Different letters indicate significant differences in the same metal(loid)s removal rate among biochar treatments ($n = 3$, $p < 0.05$).

3.2. Separation efficiency of magnetic biochar from soil

Separation of biochar from soil under magnetic field was mainly determined by the magnetism of biochar. Before the application to soil, the saturation magnetizations of three magnetized biochar were in the order of MP > PM > PMP (Fig. 3a), which changed to MP > PMP > PM after the soil removal experiment (Fig. 3b). The saturation magnetizations of the MP and PM biochars separated from soil significantly decreased, while the saturation magnetization of PMP biochar remained relatively unchanged.

The separation efficiency of biochar from soil was evaluated via the recovery rate of biochar (Fig. 3c) and the change in soil properties after the separation of biochar (Table 1). The highest recovery rate of magnetic biochar was ~65%, with PMP > PM > MP. This indicated that after the separation, the biochar: soil ratio decreased to ~3:100, and the Fe: soil ratio was ~1.2%. The properties of soil after the application and thereafter the separation of the magnetic biochar have been changed slightly, mainly in terms of clay content, TOC, nitrogen and phosphorus (Table 1).

3.3. Characteristics of the synthesized biochar

All these biochar samples possess the hierarchical porous structure, exhibiting the micro/mesopores-dominant nature of the samples (Fig. S5). The magnetizing processes led to a decrease in the surface area, which was observed for all the different pore sizes. Both the total pore volume and the micropore volume were in the order of P > PM > PMP > MP, in the same order with the carbon content, and opposite to the order of the iron content (Fe%) (Table 2).

XRD spectrum clearly indicated that Fe_3O_4 (magnetite) was incorporated on the surface of the biochar particles (Fig. 4). Peaks at 30.3°, 35.5°, 43.3°, 56.9° and 62.7° are characteristics of cubic magnetite that is described with the standard Powder Diffraction File (PDF 99-0073). PMP treatment showed the existence of a small amount of γ-Fe_2O_3 (maghemite), suggested by its brown color, unlike Fe_3O_4 (magnetite) which is black (Schwertmann and Cornell, 2000).

SEM images indicated both tubular and circular microstructures of the raw biochar (Fig. S6). After magnetization, Fe particles can be found on the surface of the three magnetic biochars. PMP treatment, after twice pyrolysis, showed a blurred edge on the tubular structure.

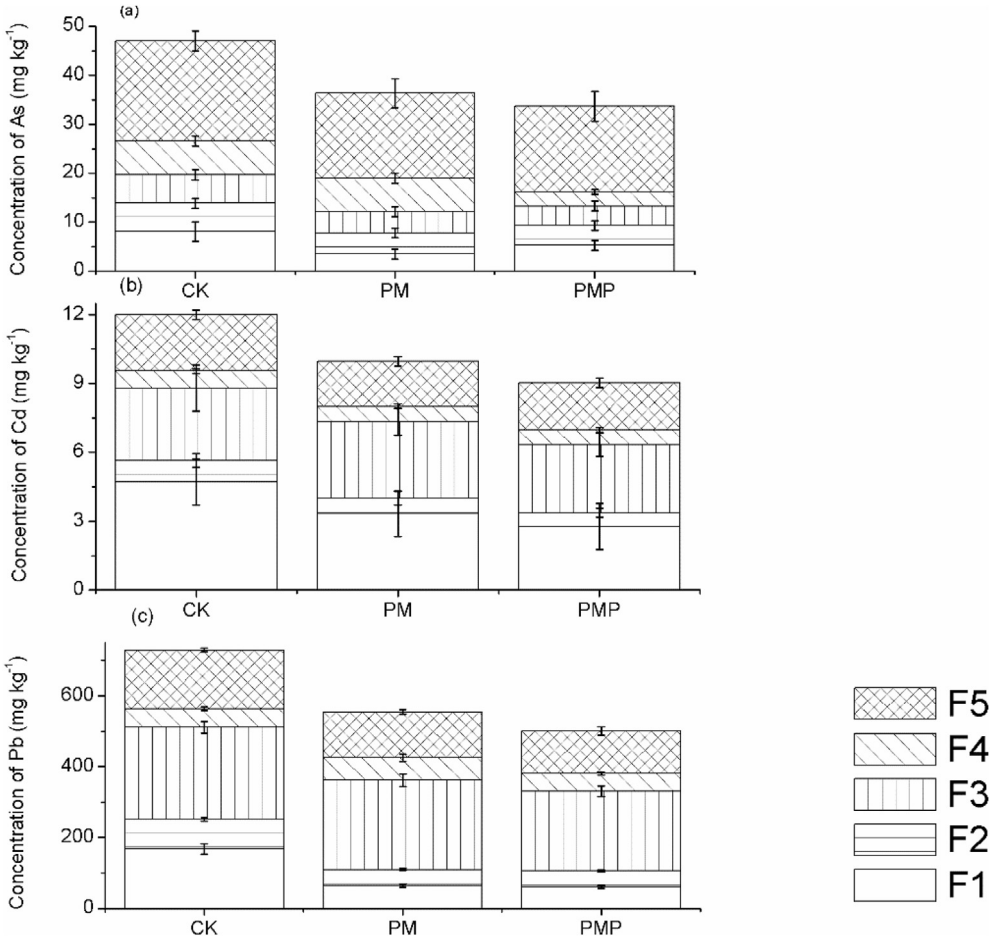

Fig. 2. Sequential extraction of As, Cd and Pb from soil under different treatments. The As fractions were categorized as F1: non-specifically sorbed; F2: specifically-sorbed; F3: amorphous and poorly-crystalline hydrous oxides of Fe and Al; F4: well-crystallized hydrous oxides of Fe and Al; and F5: residual phases. The Cd and Pb fractions were categorized as F1: extractable metals; F2: metals bound to carbonates; F3: metals bound to Fe–Mn oxides; F4: metals bound to organic matter and F5: residual phases. CK indicates the treatment with only soil, no biochar; PM indicates the biochar produced by magnetization after pyrolysis; PMP indicates the biochar produced by pyrolysis twice, once before magnetizing and again after magnetizing.

3.4. Changes in biochar characteristics after adsorption experiment

SEM-EDS further disclosed the chemical composition of biochar and Fe oxide particles on the biochar surface (Fig. 5). Before the application to soil, the PM biochar surface without Fe showed the main composition of carbon and oxygen, while the surface covered by Fe oxides showed the main composition of iron, carbon and oxygen. After the application and separation from soil, the biochar surface without Fe attached still showed a primary composition of carbon and oxygen, with some attached soil particles, evidenced via Al, Si, and a small amount of Cd and Pb. The Fe-oxides attached to the surface of the biochar had a primary composition of iron and oxygen, with attached Al, Si, and a small amount of As, Cd and Pb.

FTIR spectra indicated that for the raw biochar, peaks at 1593 cm^{-1} is characteristic for C=C in aromatic structures (Fig. 6); the band at 1030 cm^{-1} and 1053 cm^{-1} indicates the stretching vibrations of C–O–C and O–H. After the impregnation of iron oxide (PM treatment), new peaks occurred at 552 cm^{-1} and 627 cm^{-1},corresponding to the Fe–O stretching vibration of high-spin Fe^{3+} complex in Fe_3O_4. The disappearance of the peak at 1030 cm^{-1} for the PMP treatment indicated that some hydroxyls might have been lost during the second-time pyrolysis. After the soil experiment, for all the three magnetic biochars, peaks at 1030 cm^{-1} and 1007 cm^{-1} accorded with the Si–O stretching vibration of kaolinite, while peak at 910 cm^{-1} accorded with the Al_2OH bending band of kaolinite.

3.5. Micro-distribution of As on the biochar surface

XRF map found that both PM and PMP biochar separated from the As enriched solution showed an uniform distribution of Fe and As on the surface, indicating a high adsorption capacity of Fe oxides to As in the solution (Fig. 7a and c); whereas biochar separated from soil showed an uneven distribution of Fe and As (Fig. 7b and d). Additionally, a large soil particle enriched with As can be clearly seen in the XRF map of PMP biochar separated from the soil (Fig. 7d).

On As-enriched spots of untreated soil (Fig. S7a) and the soil after PMP treatment (Fig. S7b), μ-XANES spectra were obtained. Results indicated that As in the soil particles was a combination of As(III) and As(V) while the As adsorbed on the surface of biochar was mainly As(V) (Fig. S7).

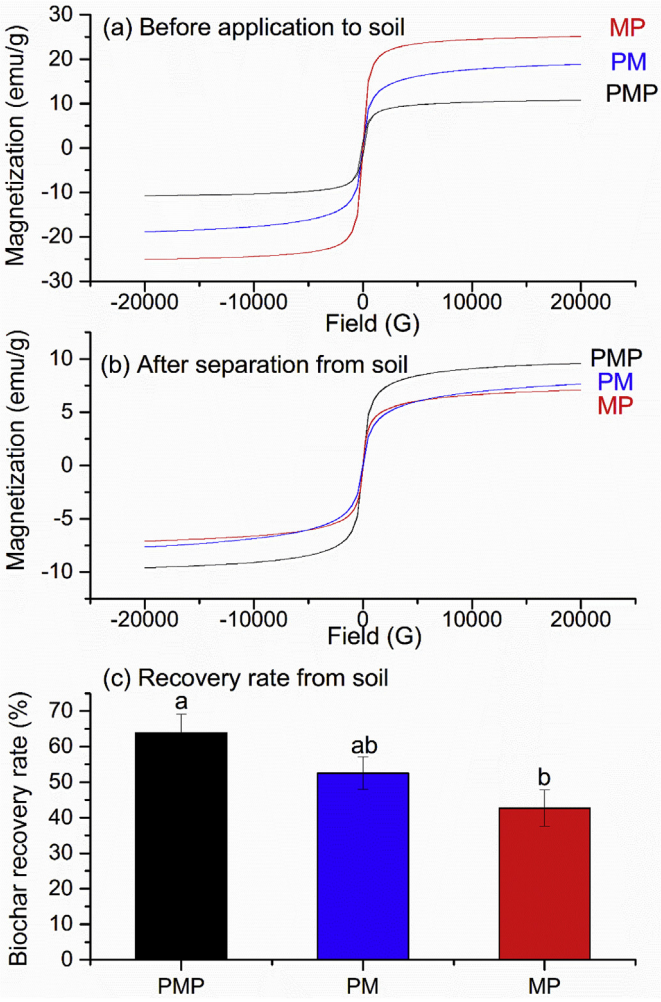

Fig. 3. Magnetic moment versus magnetic field of the magnetic biochar before (a) and after soil experiment (b), and the recovery rate of biochar from soil under magnetic field (c). PM indicates the biochar produced by magnetization after pyrolysis; MP indicates the biochar produced by pyrolyzing the magnetized biomass; PMP indicates the biochar produced by pyrolysis twice, once before magnetizing and again after magnetizing. Different letters indicate significant differences in the same metal(loid)s removal rate among biochar treatments ($n = 3$, $p < 0.05$).

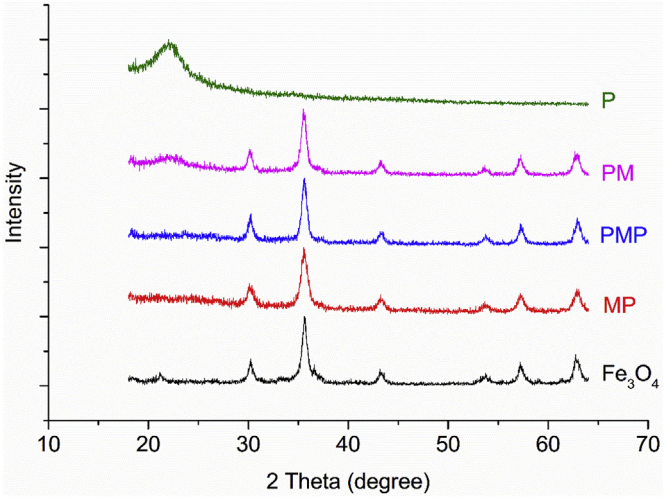

Fig. 4. XRD of the raw and magnetic biochar, and the synthesized Fe_3O_4. P indicates the biochar produced by pyrolysis only; PM indicates the biochar produced by magnetization after pyrolysis; MP indicates the biochar produced by pyrolysis the magnetized biomass; PMP indicates the biochar produced by pyrolysis twice, once before magnetizing and again after magnetizing.

4. Discussion

4.1. Removal of metal(loid)s by magnetized biochar from soil is applicable

Biochars produced by incorporating magnetic Fe oxides on the surface of biochar can simultaneously remove multiple metal(loid) contaminants from soil. In accordance with the proposed hypothesis, the incorporation of Fe on the biochar surface enabled the adsorption of As to biochar, and the separation of biochar from soil under magnetic field. One of the most surprising findings is that the Fe modified biochar not only removed soluble or exchangeable fractions of metal(loid)s from the soil, but also removed other fractions. This was evidenced both by the sequential extraction result (Fig. 2) and the SR based μ-XRF analysis (Fig. 7). As far as the authors know, this is the first report on the utilization of magnetic biochar to remove contaminants from a soil system.

One of the most used farmland remediation technology that can remove metal(loid)s from soil is phytoextraction. The reported highest As removal efficiency is ~17% per year (Chen et al., 2018b), while the Cd removal efficiency is even lower (McGrath et al., 2006). And phytoextraction usually removes one element at one time. In the current study, after incubation with the magnetized biochar for 24 h, followed by the separation of biochar from soil using a magnet, the total concentrations of As, Cd and Pb in soil decreased by 28%, 25% and 32%, respectively. Therefore, if simultaneous removal of multi-contaminants from soil is the final target, the magnetic biochar indicated a strong application potential.

Another widely used soil remediation technology is immobilization, which does not remove contaminants but decreases its transfer to other environmental media like plants and water systems. The reported immobilization ratio without affecting the growth of crops can be high for Cd but ~50% for As (Basta and McGowen, 2004; Sarkar et al., 2007). In the current study, the decrease extent of the F1 and F2 fractions of multi-metal(loid)s reached 41–64% after 24 h (Fig. 2). Therefore, the metal(loid)s immobilization efficacy of this method is also comparable to the existing technology. Unaltered biochar is a commonly used immobilizer for Cd and Pb, remaining stable even under acid rain (Lu et al., 2015). The magnetic biochar which was not removed from the soil can serve as an immobilizer for metals.

The proposed removal of metal(loid)s via magnetic biochar also has shortcomings. One of the shortcomings is that when removing the magnetic biochar from soil, some clay materials such as kaolinite were also removed. According to the FTIR spectra of biochar after soil experiment (Fig. 6), peaks at 1030 cm^{-1} and 1007 cm^{-1} accorded with the Si—O stretching vibration of kaolinite, while peak at 910 cm^{-1} accorded with the Al_2OH bending band of kaolinite (Madejová, 2003). The overall clay content decreased from 20% to 18% in all the three magnetic biochar treatments (Table 2). Although this decrease is not large, further studies are needed to evaluate the impact of this change in soil properties. Another issue is that it may be desirable to decrease the Fe dosage, considering the potential secondary contamination caused by excess Fe. In the current study, the remaining Fe content in the soil was about 1.2% by weight, which is within the range of commonly used dosages of Fe applied to soil as an As immobilizer (Fajardo et al., 2019; Zhang et al., 2010). However, toxicity symptoms of plants have been found when applying a dosage of goethite nanospheres higher than 1% by weight (Baragaño et al., 2020). Therefore, further study enabling a

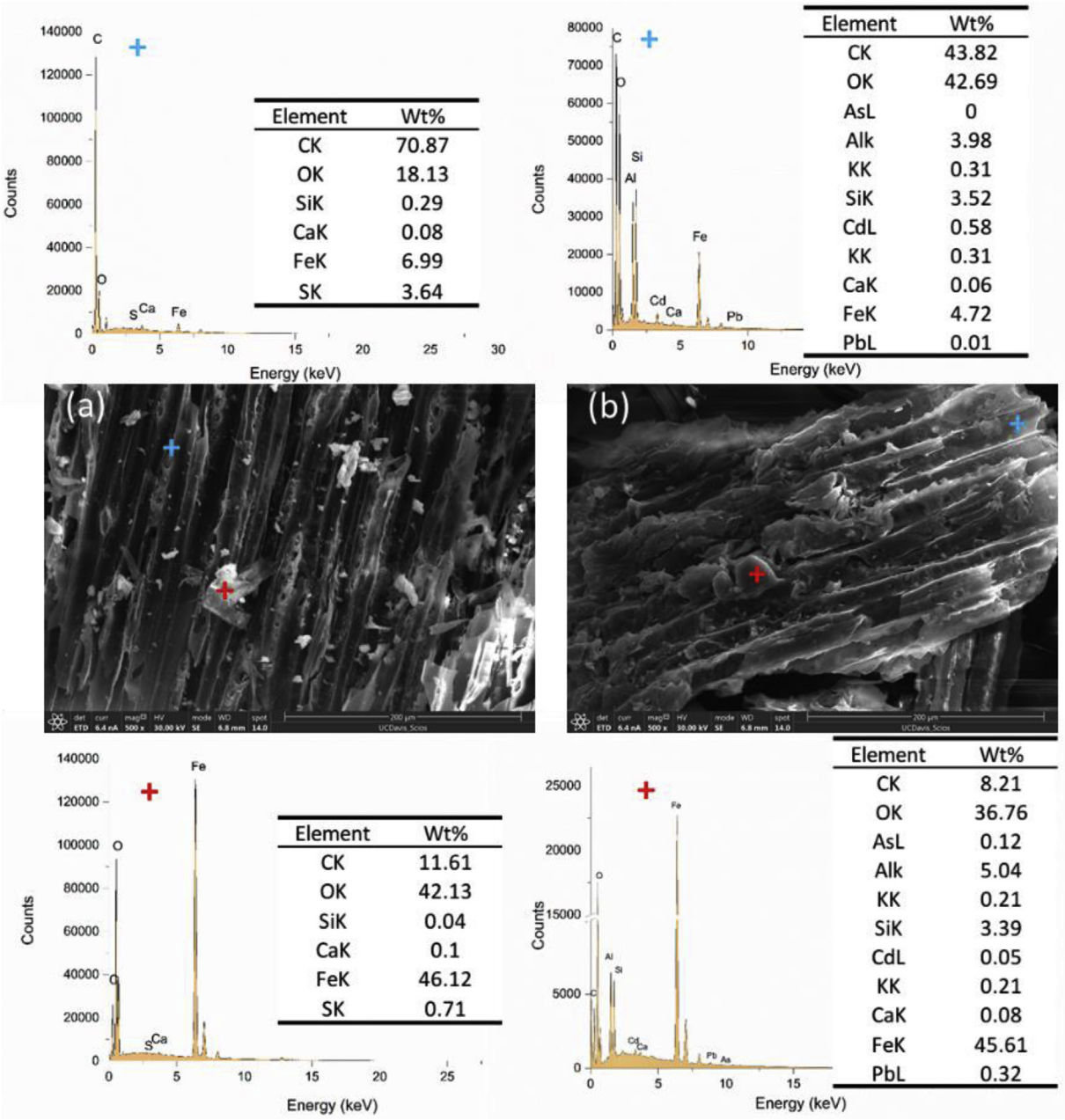

Fig. 5. SEM photo and chemical composition of PM biochar before (a) and after (b) application to soil. PM indicates the biochar produced by magnetization after pyrolysis.

decrease in the left Fe content in soil might be helpful. In addition, the efficiency of this method to soils with different contamination extents, and the possibility of a circulation process, i.e. magnetization-adsorption- demagnetization - recovery — magnetization, might worth further study.

Regardless of these issues, as a very short-term and easy-to-apply scenario, we suggest this as proof of concept for a potential contaminant removal technology.

4.2. The stability of Fe oxides on the surface of biochar determines the metal(loid)s removal efficiency

The determining factors of the metal(loid)s removal are classified into two groups, one impacting the adsorption capacity and the other related to the separation.

The adsorption of Cd and Pb depends primarily on the surface area and the pH of biochar. From the current study, it seems that pH plays a more important role than the surface area, in accordance with earlier literature (Houben et al., 2013). Although prior studies revealed that due to the catalytic effect of iron particles (Thines et al., 2017), more dehydration and decomposition of volatile matter during the pyrolysis can increase the surface area of biochar (Salimi et al., 2019), the current study found that all the three magnetizing processes decreased the surface area. The Fe particles attached to the biochar or biomass may have blocked some pores, thereby decreasing the volume of CO_2 adsorbed by the biochar in the adsorption experiment (Li et al., 2020). However, such decrease in surface area did not lower the cations adsorption capacity of biochar. On the contrary, the addition of magnetized biochar (pH ranging from 9.7 to 10.3) increased the pH value of the adsorption

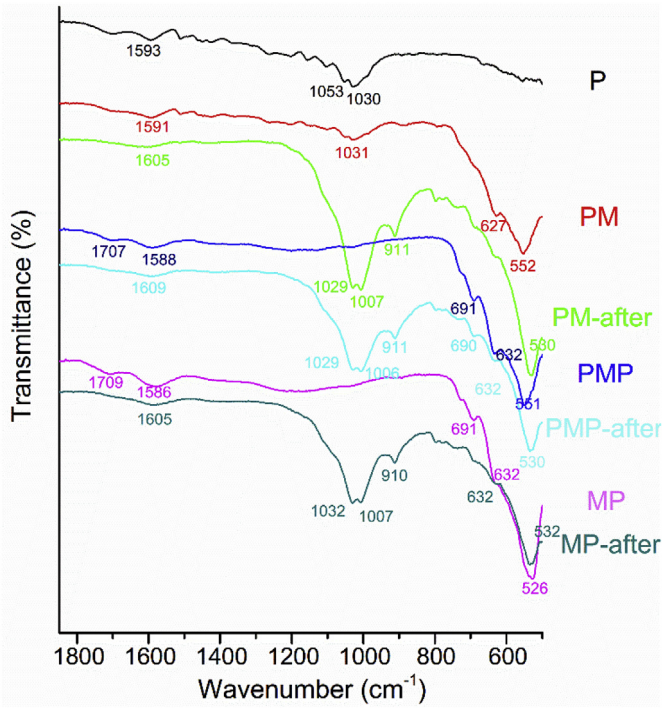

Fig. 6. FTIR spectra of biochar before and after the application of the magnetic biochar to soil. P indicates the raw biochar without magnetization; PM indicates the biochar produced by magnetization after pyrolysis; PMP indicates the biochar produced by pyrolysis twice, once before magnetizing and again after magnetizing; MP indicates the biochar produced by pyrolysis the magnetized biomass.

solution, thereby leading to a higher adsorption ability to Cd and Pb by the magnetic biochar than the raw biochar (Fig. 1b, Table 2). And based on the XRF map, there was also Cd and Pb attached to the Fe oxides. The adsorption of As mainly depends on the incorporated Fe content. Raw biochar (P treatment) can adsorb limited amount of As. The incorporation of Fe oxides on the biochar surface significantly increased the absorbed amount of As, and higher Fe content of the biochar corresponds to higher adsorption capacity of As (Fig. 1b, Table 2). Therefore, the adsorption of these three elements to magnetic biochars was in accordance with earlier literature (Wu et al., 2018). Arsenic was mainly adsorbed to Fe oxides due to electrostatic and specific adsorptions, whereas Cd/Pb was adsorbed to both Fe oxides and biochar, via electrostatic and physical adsorptions, respectively.

The separation of biochar from soil depends primarily on the magnetization ability and its stability, i.e., the magnetism of biochar after adsorption. After 24 h contact with soil, Fe oxides on the surface of PMP biochar remained magnetic while for the other two magnetic biochars, there was an apparent decrease in magnetization (Fig. 3). Among the three different magnetic biochars, PMP treatment did not have the strongest metal(loid)s adsorption capacity (Fig. 1, Figs. S2–S4), but it showed the highest removal efficiency for all the three metal(loid)s from soil slurry, which mainly came from its high stability in the soil system (Fig. 1a). Therefore, the stability of Fe oxides on the surface of biochar during soil experiment is a determining factor for the removal efficiency of metal(loid)s from soil. Iron is a redox active element in the soil, and can cycle through reduced (Fe^{2+}) and oxidized (Fe^{3+}) forms with wet-dry cycles, leading to its dissolution and re-precipitation, respectively (Suda and Makino, 2016; Yamaguchi et al., 2011). Such cycle of dissolution and re-precipitation may have decreased its separation efficiency with soil. The pyrolysis after magnetization may somehow retain magnetic Fe oxide particles in the pores of biochar, thereby preventing the loss of magnetism. In addition, there was a transformation of Fe_3O_4 to γ-Fe_2O_3 during the second pyrolysis of the PMP treatment, suggested by its brown color (Schwertmann and Cornell, 2000). Although the furnace was filled with N_2 atmosphere, perhaps there was some oxidation reactions during the magnetizing and drying process. Considering the similar magnetic properties of γ-Fe_2O_3 with Fe_3O_4 and the better chemical stability of γ-Fe_2O_3 than Fe_3O_4 (Sun et al., 2004), such transformation might also contribute to the higher stability of Fe oxides in the PMP treatment.

The micro-XRF map of biochar separated from soil experiment found an As-enriched soil particle (Fig. 7). Due to the significant correlation between soil magnetic susceptibility and soil heavy metal content under many cases (Ayoubi and Karami, 2019), magnetic susceptibility can indirectly reflect the heavy metal contamination of soil as it is influenced both anthropogenically and naturally by lithological and pedological heavy metal content (Liu et al., 2016). In the soil, a considerable amount of metal(loid)s was attached to Fe/Mn oxides (Sungur et al., 2014). Percentage of As, Cd and Pb attached to Fe/Mn oxides in the current soil was about 26%, 25% and 31%, respectively (Fig. 2). Therefore, it is suggested that due to the common source of heavy metals and Fe/Mn oxides and their strong tendency to combine with each other, some solid particles containing high concentrations of As were directly attached to magnetic biochars, favoring its removal.

μ-XANES revealed that after the soil experiment, As on the biochar surface was only As(V) while before the soil experiment there was a mix of As(III) and As(V). (Fig. S7). This could be attributed to the selective adsorption of Fe oxides to As(V) and the oxidation reaction of As(III) to As(V) on the surface of the biochar. Under reducing conditions, the dissolution and re-precipitation process of Fe often leads to the formation of amorphous Fe oxides, which can adsorb an increased amount of As from soil (Liu et al., 2015). Therefore, we suggest three possible processes attaching As in soil to the magnetic biochar: (1) direct attachment of As-enriched magnetic soil particles; (2) dissolution of Fe and the associated oxidization of As(III) to As(V), and (3) adsorption or precipitation of As(V) to amorphous Fe oxides under reducing conditions.

The Fe/C ratio of the three magnetic biochars was different, which came from both the pyrolysis and the magnetifying procedures, including the pyrolysis time, and the initial input of biomass and Fe oxides. The comparison with an increased number of treatments considering more affecting factors, might be helpful to optimize the producing procedures of magnetic biochar. Pyrolysis temperature is another factor impacting the adsorption of metal(loid)s to biochar. Generally, higher pyrolysis temperature increases the biochar surface area, favoring the adsorption of contaminants, such as Cd and Pb in form of cations (Li et al., 2020). Biochars produced under high pyrolysis temperature of 600 °C, or higher, have been found to efficiently remove metals or degrade organics from water (Sun et al., 2019; Yang et al., 2018). However, for As oxyanions, the liming effect brought in by high pyrolysis temperature decreased the As adsorption. In the current study, low pyrolysis temperature favoring As adsorption was adopted (Fig. S1). Further optimization of pyrolysis temperatures of the two pyrolysis reactions during producing processes of PMP treatment might further improve the metal(loid)s removal efficiency.

5. Conclusions

Magnetic biochar with benefits of both biochar and Fe oxides can simultaneously remove multiple metal(loid) contaminants from soil. After the application and separation of the magnetic

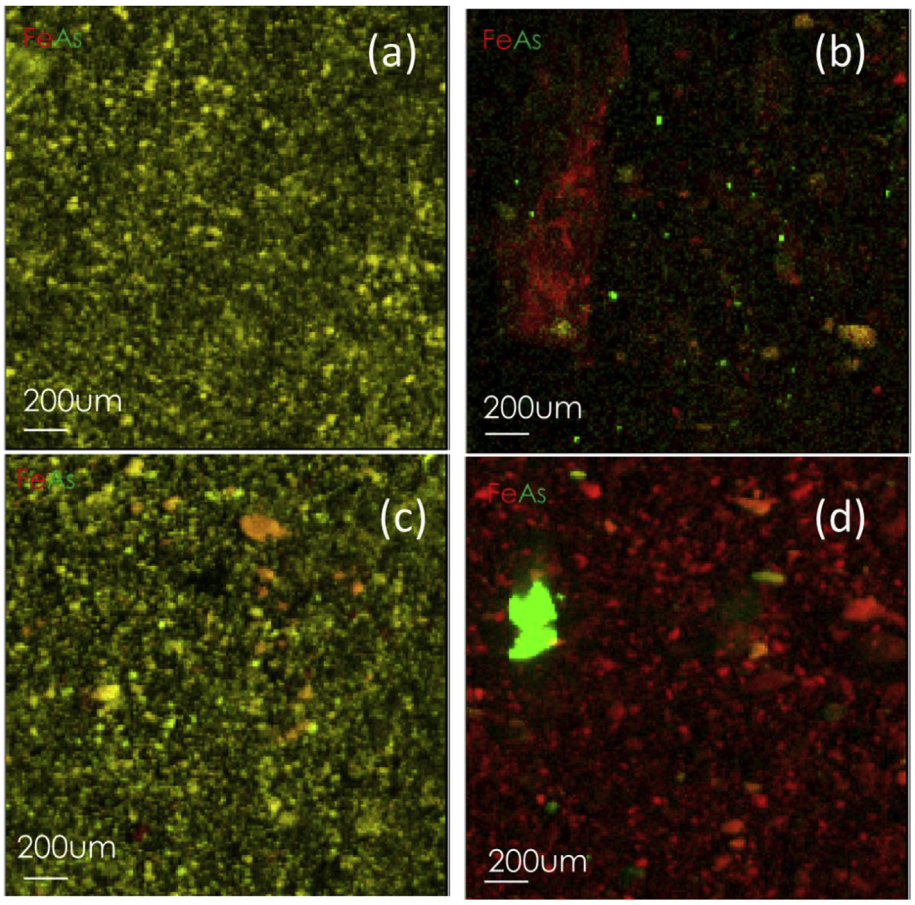

Fig. 7. XRF map of PM biochar separated from aqueous system (a) and soil system (b), and PMP biochar separated from aqueous system (c) and soil system (d). PM indicates the biochar produced by magnetization after pyrolysis; PMP indicates the biochar produced by pyrolysis twice, once before magnetizing and again after magnetizing.

biochar, the total concentrations of As, Cd and Pb in soil decreased by 28%, 25% and 32%, respectively. Not only the soluble and exchangeable fractions of metal(loid)s can be removed, the solid fractions can also be directly adsorbed to biochar. In addition, unlike water treatment, the stability of the magnetic biochar is a determining factor for soil treatment. Further study on the dynamic change in Fe speciation after the application of Fe modified biochar to soil, and its relationship with the speciation of As, may further aid the optimization of adsorbents producing procedures.

CRediT authorship contribution statement

Xiaoming Wan: Conceptualization, Methodology, Investigation, Writing - original draft, Project administration, Funding acquisition. **Chongyang Li:** Methodology, Investigation, Writing - review & editing. **Sanjai J. Parikh:** Conceptualization, Writing - review & editing, Supervision.

Acknowledgements

Financial support was provided by the National Key Research and Development Program of China (Grant No. 2018YFC1800302), the Youth Innovation Promotion Association of the Chinese Academy of Sciences (No. 2017075), and China Scholarship Council (CSC). Dr. Sirine Fakra from Beamline 10.3.2 Advanced Light Source, Lawrence Berkeley National Lab, has provided kind help when we conduct Micro-XRF and XANES experiment there. Dr. Kyle Leach from Sierra Streams Institute has provided contaminated soil used in the study.

Appendix A. Supplementary data

Supplementary data to this article can be found online at https://doi.org/10.1016/j.envpol.2020.114157.

References

Ayoubi, S., Karami, M., 2019. Pedotransfer functions for predicting heavy metals in natural soils using magnetic measures and soil properties. J. Geochem. Explor. 197, 212–219.
Baragaño, D., Alonso, J., Gallego, J.R., Lobo, M.C., Gil-Díaz, M., 2020. Zero valent iron and goethite nanoparticles as new promising remediation techniques for As-polluted soils. Chemosphere 238, 124624.
Basta, N.T., McGowen, S.L., 2004. Evaluation of chemical immobilization treatments for reducing heavy metal transport in a smelter-contaminated soil. Environ. Pollut. 127, 73–82.
Beesley, L., Marmiroli, M., 2011. The immobilisation and retention of soluble arsenic, cadmium and zinc by biochar. Environ. Pollut. 159, 474–480.
Beesley, L., Moreno-Jimenez, E., Gomez-Eyles, J.L., Harris, E., Robinson, B., Sizmur, T., 2011. A review of biochars' potential role in the remediation, revegetation and restoration of contaminated soils. Environ. Pollut. 159, 3269–3282.
Chen, L., Zhou, S.L., Wu, S.H., Wang, C.H., Li, B.J., Li, Y., Wang, J.X., 2018a. Combining emission inventory and isotope ratio analyses for quantitative source apportionment of heavy metals in agricultural soil. Chemosphere 204, 140–147.
Chen, T., Lei, M., Wan, X., Yang, J., Zhou, X., 2018b. Arsenic hyperaccumulator pteris vittata L. And its application to the field. In: Luo, Y., Tu, C. (Eds.), Twenty Years of Research and Development on Soil Pollution and Remediation in China. Springer Singapore, Singapore, pp. 465–476.
de Abreu, C.A., Coscione, A.R., Pires, A.M., Paz-Ferreiro, J., 2012. Phytoremediation of a soil contaminated by heavy metals and boron using castor oil plants and organic matter amendments. J. Geochem. Explor. 123, 3–7.
Fajardo, C., Costa, G., Nande, M., Martín, C., Martín, M., Sánchez-Fortún, S., 2019.

Heavy metals immobilization capability of two iron-based nanoparticles (nZVI and Fe3O4): soil and freshwater bioassays to assess ecotoxicological impact. Sci. Total Environ. 656, 421–432.
Gelardi, D.L., Li, C., Parikh, S.J., 2019. An emerging environmental concern: biochar-induced dust emissions and their potentially toxic properties. Sci. Total Environ. 678, 813–820.
Gil, C., Boluda, R., Martin, J.A.R., Guzman, M., del Moral, F., Ramos-Miras, J., 2018. Assessing soil contamination and temporal trends of heavy metal contents in greenhouses on semiarid land. Land Degrad. Dev. 29, 3344–3354.
Gonçalves, S.P.c.C., Strauss, M., Martinez, D.S.T., 2018. The positive fate of biochar addition to soil in the degradation of PHBV-Silver nanoparticle composites. Environ. Sci. Technol. 52, 13845–13853.
HERO, 2016. California Department of Toxic Subtances Control. HHRA Note Number 3, DTSC-Modified Screening Levels (DTSC-SLs).
Houben, D., Evrard, L., Sonnet, P., 2013. Mobility, bioavailability and pH-dependent leaching of cadmium, zinc and lead in a contaminated soil amended with biochar. Chemosphere 92, 1450–1457.
Igalavithana, A.D., Kim, K.-H., Jung, J.-M., Heo, H.-S., Kwon, E.E., Tack, F.M.G., Tsang, D.C.W., Jeon, Y.J., Ok, Y.S., 2019. Effect of biochars pyrolyzed in N2 and CO2, and feedstock on microbial community in metal(loid)s contaminated soils. Environ. Int. 126, 791–801.
Khalid, S., Shahid, M., Niazi, N.K., Murtaza, B., Bibi, I., Dumat, C., 2017. A comparison of technologies for remediation of heavy metal contaminated soils. J. Geochem. Explor. 182, 247–268.
Kim, K.-W., Bang, S., Zhu, Y., Meharg, A.A., Bhattacharya, P., 2009. Arsenic geochemistry, transport mechanism in the soil–plant system, human and animal health issues. Environ. Int. 35, 453–454.
Kolhatkar, A.G., Chen, Y.-T., Chinwangso, P., Nekrashevich, I., Dannangoda, G.C., Singh, A., Jamison, A.C., Zenasni, O., Rusakova, I.A., Martirosyan, K.S., Litvinov, D., Xu, S., Willson, R.C., Lee, T.R., 2017. Magnetic sensing potential of Fe3O4 nanocubes exceeds that of Fe3O4 nanospheres. ACS Omega 2, 8010–8019.
Komarek, M., Vanek, A., Ettler, V., 2013. Chemical stabilization of metals and arsenic in contaminated soils using oxides - a review. Environ. Pollut. 172, 9–22.
Kumar, P., Dushenkov, V., Motto, H., Raskin, I., 1995. Phytoextraction - the use of plants to remove heavy-metals from soils. Environ. Sci. Technol. 29, 1232–1238.
Li, C., Bair, D.A., Parikh, S.J., 2018. Estimating potential dust emissions from biochar amended soils under simulated tillage. Sci. Total Environ. 625, 1093–1101.
Li, S.-W., Sun, H.-J., Li, H.-B., Luo, J., Ma, L.Q., 2016. Assessment of cadmium bioaccessibility to predict its bioavailability in contaminated soils. Environ. Int. 94, 600–606.
Li, Z., Sun, Y., Yang, Y., Han, Y., Wang, T., Chen, J., Tsang, D.C.W., 2020. Biochar-supported nanoscale zero-valent iron as an efficient catalyst for organic degradation in groundwater. J. Hazard Mater. 383, 121240.
Liu, C.P., Yu, H.Y., Liu, C.S., Lie, F.B., Xu, X.H., Wang, Q., 2015. Arsenic availability in rice from a mining area: is amorphous iron oxide-bound arsenic a source or sink? Environ. Pollut. 199, 95–101.
Liu, D., Ma, J., Sun, Y., Li, Y., 2016. Spatial distribution of soil magnetic susceptibility and correlation with heavy metal pollution in Kaifeng City, China. Catena 139, 53–60.
Lu, H., Li, Z., Fu, S., Méndez, A., Gascó, G., Paz-Ferreiro, J., 2015. Effect of biochar in cadmium availability and soil biological activity in an anthrosol following acid rain deposition and aging. Water, Air, Soil Pollut. 226, 164.
Lu, H.P., Li, Z.A., Gascó, G., Méndez, A., Shen, Y., Paz-Ferreiro, J., 2018. Use of magnetic biochars for the immobilization of heavy metals in a multi-contaminated soil. Sci. Total Environ. 622–623, 892–899.
Madejová, J., 2003. FTIR techniques in clay mineral studies. Vib. Spectrosc. 31, 1–10.
McGrath, S.P., Lombi, E., Gray, C.W., Caille, N., Dunham, S.J., Zhao, F.J., 2006. Field evaluation of Cd and Zn phytoextraction potential by the hyperaccumulators Thlaspi caerulescens and Arabidopsis halleri. Environ. Pollut. 141, 115–125.
Mukome, F.N.D., Zhang, X., Silva, L.C.R., Six, J., Parikh, S.J., 2013. Use of chemical and physical characteristics to investigate trends in biochar feedstocks. J. Agric. Food Chem. 61, 2196–2204.
Netherway, P., Reichman, S.M., Laidlaw, M., Scheckel, K., Pingitore, N., Gascó, G., Méndez, A., Surapaneni, A., Paz-Ferreiro, J., 2019. Phosphorus-rich biochars can transform lead in an urban contaminated soil. J. Environ. Qual. 48, 1091–1099.
Norton, G.J., Williams, P.N., Adomako, E.E., Price, A.H., Zhu, Y., Zhao, F.-J., McGrath, S., Deacon, C.M., Villada, A., Sommella, A., Lu, Y., Ming, L., De Silva, P.M.C.S., Brammer, H., Dasgupta, T., Islam, M.R., Meharg, A.A., 2014. Lead in rice: analysis of baseline lead levels in market and field collected rice grains. Sci. Total Environ. 485–486, 428–434.
O'Connor, D., Peng, T.Y., Zhang, J.L., Tsang, D.C.W., Alessi, D.S., Shen, Z.T., Bolan, N.S., Hou, D.Y., 2018. Biochar application for the remediation of heavy metal polluted land: a review of in situ field trials. Sci. Total Environ. 619, 815–826.
Palansooriya, K.N., Shaheen, S.M., Chen, S.S., Tsang, D.C.W., Hashimoto, Y., Hou, D., Bolan, N.S., Rinklebe, J., Ok, Y.S., 2020. Soil amendments for immobilization of potentially toxic elements in contaminated soils: a critical review. Environ. Int. 134, 105046.
Qiao, J.T., Liu, T.X., Wang, X.Q., Li, F.B., Lv, Y.H., Cui, J.H., Zeng, X.D., Yuan, Y.Z., Liu, C.P., 2018. Simultaneous alleviation of cadmium and arsenic accumulation in rice by applying zero-valent iron and biochar to contaminated paddy soils. Chemosphere 195, 260–271.
Rai, P.K., Lee, S.S., Zhang, M., Tsang, Y.F., Kim, K.H., 2019. Heavy metals in food crops: health risks, fate, mechanisms, and management. Environ. Int. 125, 365–385.
Salimi, P., Norouzi, O., Pourhoseini, S.E.M., Bartocci, P., Tavasoli, A., Di Maria, F., Pirbazari, S.M., Bidini, G., Fantozzi, F., 2019. Magnetic biochar obtained through catalytic pyrolysis of macroalgae: a promising anode material for Li-ion batteries. Renew. Energy 140, 704–714.
Sarkar, D., Makris, K.C., Vandanapu, V., Datta, R., 2007. Arsenic immobilization in soils amended with drinking-water treatment residuals. Environ. Pollut. 146, 414–419.
Schwertmann, U., Cornell, R.M., 2000. Iron Oxides in the Laboratory: Preparation and Characterization, second ed. Wiley-VCH, Weinheim, Germany.
Shajib, M.T.I., Hansen, H.C.B., Liang, T., Holm, P.E., 2019. Metals in surface specific urban runoff in Beijing. Environ. Pollut. 248, 584–598.
Suda, A., Makino, T., 2016. Functional effects of manganese and iron oxides on the dynamics of trace elements in soils with a special focus on arsenic and cadmium: a review. Geoderma 270, 68–75.
Sun, Y.-k., Ma, M., Zhang, Y., Gu, N., 2004. Synthesis of nanometer-size maghemite particles from magnetite. Colloid. Surface. Physicochem. Eng. Aspect. 245, 15–19.
Sun, Y., Yu, I.K.M., Tsang, D.C.W., Cao, X., Lin, D., Wang, L., Graham, N.J.D., Alessi, D.S., Komárek, M., Ok, Y.S., Feng, Y., Li, X.-D., 2019. Multifunctional iron-biochar composites for the removal of potentially toxic elements, inherent cations, and hetero-chloride from hydraulic fracturing wastewater. Environ. Int. 124, 521–532.
Sungur, A., Soylak, M., Yilmaz, E., Yilmaz, S., Ozcan, H., 2014. Characterization of heavy metal fractions in agricultural soils by sequential extraction procedure: the relationship between soil properties and heavy metal fractions. Soil Sediment Contam.: Int. J. 24, 1–15.
Tessier, A., Campbell, P.G.C., Bisson, M., 1979. Sequential extraction procedure for the speciation of particulate trace-metals. Anal. Chem. 51, 844–851.
Thines, K.R., Abdullah, E.C., Mubarak, N.M., Ruthiraan, M., 2017. In-situ polymerization of magnetic biochar – polypyrrole composite: a novel application in supercapacitor. Biomass Bioenergy 98, 95–111.
Tian, S.H., Liang, T., Li, K.X., 2019. Fine road dust contamination in a mining area presents a likely air pollution hotspot and threat to human health. Environ. Int. 128, 201–209.
Toth, G., Hermann, T., Da Silva, M.R., Montanarella, L., 2016. Heavy metals in agricultural soils of the European Union with implications for food safety. Environ. Int. 88, 299–309.
Vitkova, M., Rakosova, S., Michalkova, Z., Komarek, M., 2017. Metal(loid)s behaviour in soils amended with nano zero-valent iron as a function of pH and time. J. Environ. Manag. 186, 268–276.
Wenzel, W.W., Kirchbaumer, N., Prohaska, T., Stingeder, G., Lombi, E., Adriano, D.C., 2001. Arsenic fractionation in soils using an improved sequential extraction procedure. Anal. Chim. Acta 436, 309–323.
Wiedemeier, D.B., Hilf, M.D., Smittenberg, R.H., Haberle, S.G., Schmidt, M.W.I., 2013. Improved assessment of pyrogenic carbon quantity and quality in environmental samples by high-performance liquid chromatography. J. Chromatogr. A 1304, 246–250.
Wu, J., Huang, D., Liu, X., Meng, J., Tang, C., Xu, J., 2018. Remediation of As(III) and Cd(II) co-contamination and its mechanism in aqueous systems by a novel calcium-based magnetic biochar. J. Hazard Mater. 348, 10–19.
Xing, Y., Wang, J., Shaheen, S.M., Feng, X., Chen, Z., Zhang, H., Rinklebe, J., 2019. Mitigation of mercury accumulation in rice using rice hull-derived biochar as soil amendment: a field investigation. J. Hazard Mater. 121747.
Yamaguchi, N., Nakamura, T., Dong, D., Takahashi, Y., Amachi, S., Makino, T., 2011. Arsenic release from flooded paddy soils is influenced by speciation, Eh, pH, and iron dissolution. Chemosphere 83, 925–932.
Yang, F., Zhang, S., Sun, Y., Cheng, K., Li, J., Tsang, D.C.W., 2018. Fabrication and characterization of hydrophilic corn stalk biochar-supported nanoscale zero-valent iron composites for efficient metal removal. Bioresour. Technol. 265, 490–497.
Zhang, M., Gao, B., Varnoosfaderani, S., Hebard, A., Yao, Y., Inyang, M., 2013. Preparation and characterization of a novel magnetic biochar for arsenic removal. Bioresour. Technol. 130, 457–462.
Zhang, M., Wang, Y., Zhao, D., Pan, G., 2010. Immobilization of arsenic in soils by stabilized nanoscale zero-valent iron, iron sulfide (FeS), and magnetite (Fe3O4) particles. Chin. Sci. Bull. 55, 365–372.
Zhang, P., O'Connor, D., Wang, Y., Jiang, L., Xia, T., Wang, L., Tsang, D.C.W., Ok, Y.S., Hou, D., 2020. A green biochar/iron oxide composite for methylene blue removal. J. Hazard Mater. 384, 121286.